Supporting information

Optimization the Sensing Performance of $BaTiO_3$/P(VDF-TrFE) via Proton Irradiation

*Jie Peng[1 #], Xiaoyu Pan[2 #], Pengfei Hou[1 *] and Bo Li[3, 4 *]*

[1] *Key Laboratory of Materials Design and Preparation Technology of Hunan Province, School of Materials Science and Engineering, Xiangtan University, Hunan Xiangtan 411105, China*

[2] *College of Integrated Circuits, Nanjing University of Aeronautics and Astronautics, and Key Laboratory of Aerospace Integrated Circuits and Microsystem, Ministry of Industry and Information Technology, Nanjing 211106, China*

[3] *College of Electrical, Energy and Power Engineering, Yangzhou University, Yangzhou, 225127, China*

[4] *Department of Materials Science and Engineering, Southern University of Science and Technology, Shenzhen, Guangdong 518055, China.*

(houpf@xtu.edu.cn; bli6@yzu.edu.cn)

Discussion

1.Response mechanism of pyroelectric current in composite films

When the temperature rises ($\mathrm{d}T/\mathrm{d}t>0$), the intense electric dipole oscillations lead to a decrease in the spontaneous polarization of P(VDF-TrFE), the pyroelectric current decreases after reaching its maximum value during the heating process. Conversely, when the temperature decreases ($\mathrm{d}T/\mathrm{d}t<0$), the electric dipole oscillations weaken, and the spontaneous polarization increases and the pyroelectric current increases in reverse[1].

2.The pyroelectric coefficient of composite film obtains for experimental

The pyroelectric coefficient (p) plays a crucial role in evaluating the sensitivity and response speed of pyroelectric materials. The pyroelectric coefficient of the composite film can be determined by the following equation[2-3]:

$$p = I/[A\cdot(\mathrm{d}T/\mathrm{d}t)] \tag{1}$$

where I is pyroelectric current, $\mathrm{d}T/\mathrm{d}t$ represents the temperature change and A denotes the electrode area.

3.Calculation of pyroelectric voltage output of the devices and coefficient of determination

The pyroelectric voltage output of the devices $S_\mathrm{t}=\Delta V_\mathrm{t}/\Delta T$, where ΔV_t and ΔT are the relative change of pyroelectric voltage output and temperature, respectively. R^2 in the manuscript indicates the degree of fit of the trend line indicator, and its numerical magnitude reflects the degree of fit between the estimated value of the trend line and the corresponding actual data. The higher the degree of fit, the more reliable the trend line is. The R^2 value is calculated as follows[4]:

$$R^2 = \frac{SSR}{SST} = \frac{\sum_{i=1}^{n} (\hat{y}_i - \bar{y})^2}{\sum_{i=1}^{n} (y_i - \bar{y})^2} \tag{2}$$

Where $\hat{y}_i$ is the voltage, and $\bar{y}$ is the average voltage.

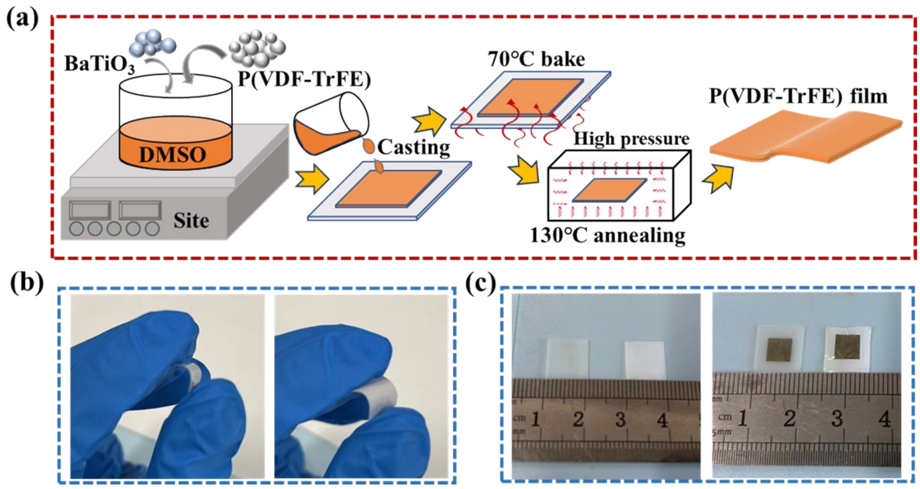

Fig. S1. (a) Preparation process of the composite film. (b) Flexibility of the composite films. (c) Optical images of the films before (left) and after (right) sputtering electrode.

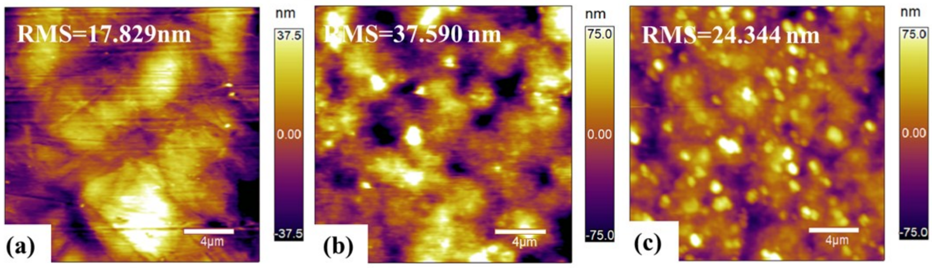

Fig. S2. Atomic force microscopy (AFM) morphology of intrinsic P(VDF-TrFE) film (a), 2wt% (b) and 4wt% (c) $BaTiO_3$/P(VDF-TrFE) composite films.

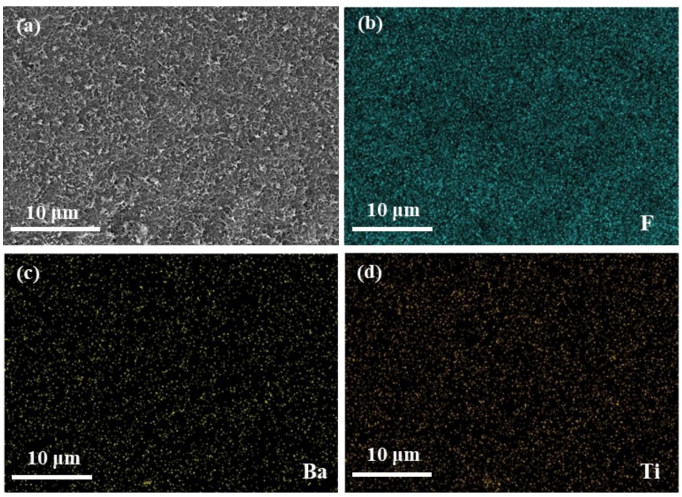

Fig. S3. (a) SEM Scanning electron microscopy (SEM) image of 2wt% $BaTiO_3$/P(VDF-TrFE) composite film. (b-d) Energy Dispersive Spectroscopy (EDS) elemental mapping images of the composite film, corresponding to F (b), Ba (c) and Ti (d).

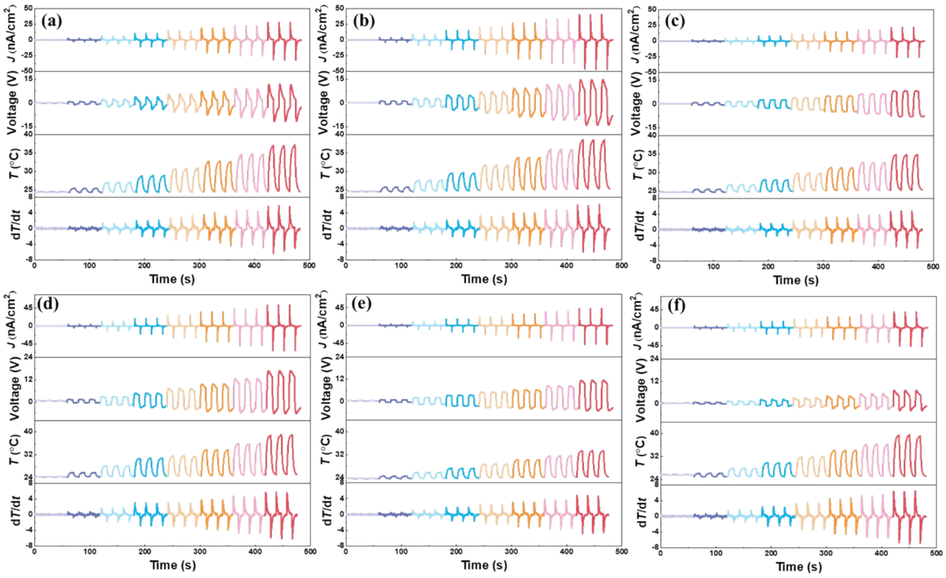

Fig. S4. (a-c) Pyroelectric response curve of intrinsic P(VDF-TrFE) film (a), 2wt% (b), and 4wt% (c) $BaTiO_3$/P(VDF-TrFE) composite films. (d-f) Pyroelectric response curve of 2wt% $BaTiO_3$/P(VDF-TrFE) composite films after irradiation with fluences of 1×10^{10} p/cm^2 (d), 5×10^{10} p/cm^2 (e) and 1×10^{11} p/cm^2 (f).

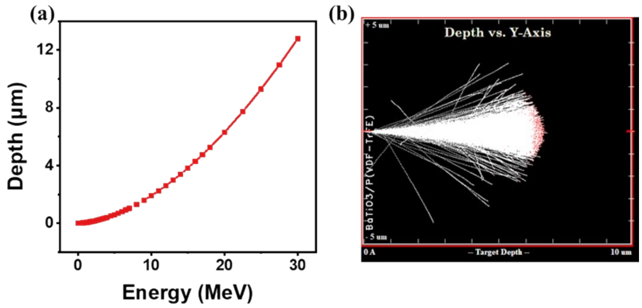

Fig. S5. (a) Proton penetration depth in the films with different incident proton energies. (b) Irradiation depth of the film under 20 MeV proton irradiation.

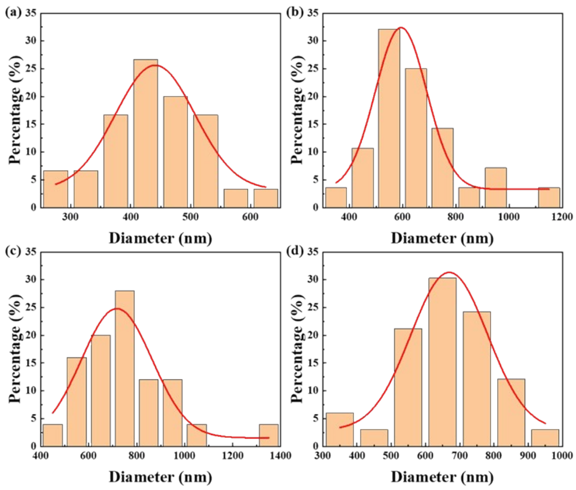

Fig. S6. *(*a) Particle size distribution histogram of 2wt% $BaTiO_3$/P(VDF-TrFE) composite film. (b-d) Particle size distribution histograms of 2wt% $BaTiO_3$/P(VDF-TrFE) composite film after irradiation with fluences of 1×10^{10} p/cm^2 (b), 5×10^{10} p/cm^2 (c), and 1×10^{11} p/cm^2 (d).

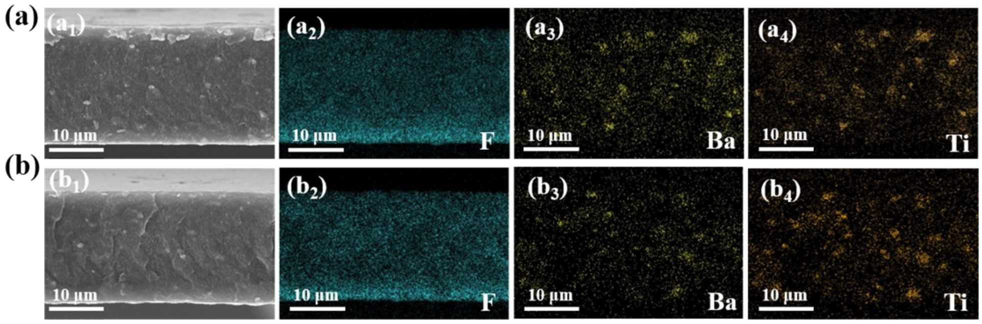

Fig. S7. (a) SEM image of 2wt% $BaTiO_3$/P(VDF-TrFE) composite film at the irradiation fluence of 5×10^{10} p/cm^2 (a_1), EDS elemental mapping images of the composite film, corresponding to F (a_2), Ba (a_3) and Ti (a_4). (b) SEM image of 2wt% $BaTiO_3$/P(VDF-TrFE) composite film at the irradiation fluence of 1×10^{11} p/cm^2 (b_1), EDS elemental mapping images of the composite film, corresponding to F (b_2), Ba (b_3) and Ti (b_4).

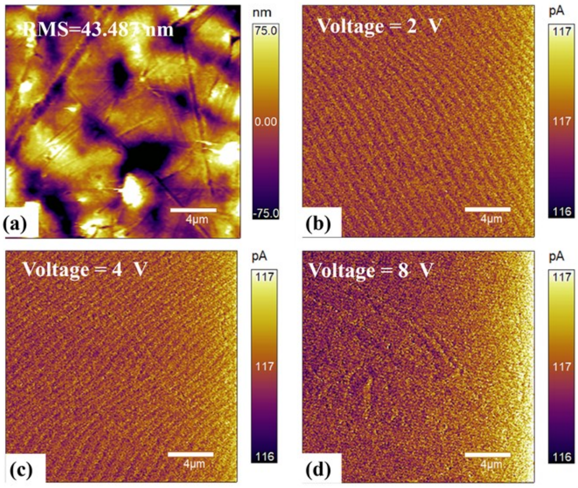

Fig. S8. (a) Morphology of 2wt% $BaTiO_3$/P(VDF-TrFE) composite film after irradiation with a fluence of 1×10^{10} p/cm^2. (b-d) Conductive atomic force microscopy (C-AFM) images of the films at applied voltages of 2 V, 4 V and 8 V.

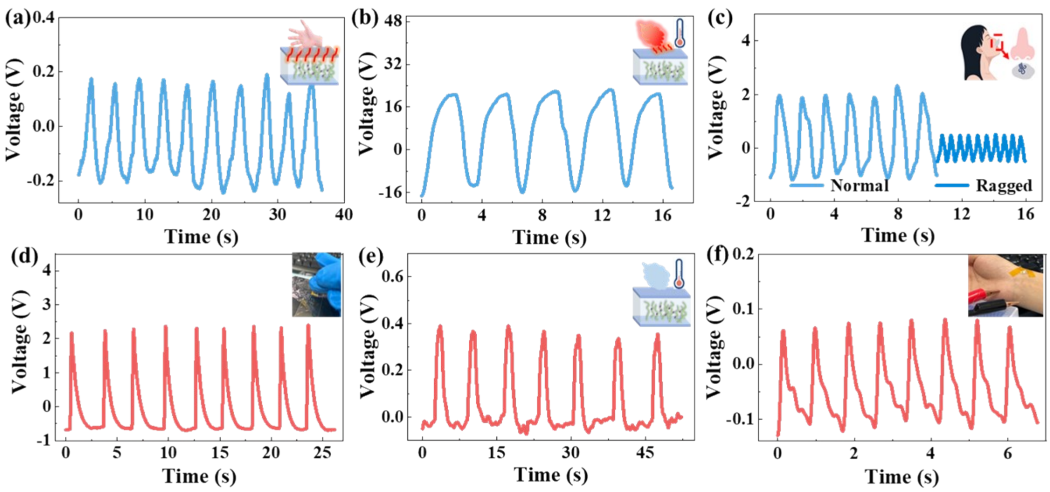

Fig. S9. The output voltage of palm thermal (a), hot air (b) breathing (c), finger press (d), cold air (e) and pulse (f).

Table S1. Lattice constants of 2wt% $BaTiO_3$/P (VDF-TrFE) composite films before and after proton irradiation.

Irradiation fluence	Lattice constant
0 p/cm^2	0.402 nm
1×10^{10} p/cm^2	0.403 nm
5×10^{10} p/cm^2	0.404 nm
1×10^{11} p/cm^2	0.404 nm

Supporting references

[1] C. Cai, H. Zhang, B. Li, Z. Han, F. Wang, P. Hou and W. Liu, *Adv. Electron. Mater.*, 2023, **9**, 2201084.

[2] G. Prestopino, R. Pezzilli, N. J. Calavita, C. Leonardi, C. Falconi and P. G. Medaglia, *Nano Energy*, 2023, **118**, 109017.

[3] A. Mohammadnia and A. Rezania, *Energ. Convers. Manage.*, 2023, **290**, 117233.

[4] B. Li, C. Cai, Y. Liu, F. Wang, B. Yang, Q. Li, P. Zhang, B. Deng, P. Hou and W. Liu, *Nat. Commun.*, 2023, **14**, 4000.